

Aminoferrocene-Based Prodrugs Activated by Reactive Oxygen Species

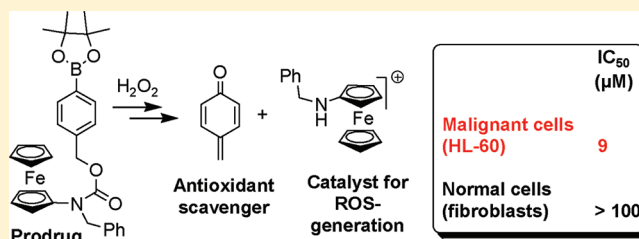
Helen Hagen,^{†,§} Paul Marzenell,^{†,§} Elmar Jentzsch,[†] Frederik Wenz,[‡] Marlon R. Veldwijk,[‡] and Andriy Mokhir^{*,†}

[†]Institute of Inorganic Chemistry, Ruprecht-Karls-University of Heidelberg, Im Neuenheimer Feld 270, 69120 Heidelberg, Germany

[‡]Department of Radiation Oncology, University Medicine Mannheim, Theodor-Kutzer-Ufer 1-3, 68167 Mannheim, Germany

S Supporting Information

ABSTRACT: Cancer cells generally generate higher amounts of reactive oxygen species than normal cells. On the basis of this difference, prodrugs have been developed (e.g., hydroxyferrocifen), which remain inactive in normal cells, but become activated in cancer cells. In this work we describe novel aminoferrocene-based prodrugs, which, in contrast to hydroxyferrocifen, after activation form not only quinone methides (QMs), but also catalysts (iron or ferrocenium ions). The released products act in a concerted fashion. In particular, QMs alkylate glutathione, thereby inhibiting the antioxidative system of the cell, whereas the iron species induce catalytic generation of hydroxyl radicals. Since the catalysts are formed as products of the activation reaction, it proceeds autocatalytically. The most potent prodrug described here is toxic toward cancer cells (human promyelocytic leukemia (HL-60), $IC_{50} = 9 \mu M$, and human glioblastoma-astrocytoma (U373), $IC_{50} = 25 \mu M$), but not toxic (up to $100 \mu M$) toward representative nonmalignant cells (fibroblasts).



system of the cell, whereas the iron species induce catalytic generation of hydroxyl radicals. Since the catalysts are formed as products of the activation reaction, it proceeds autocatalytically. The most potent prodrug described here is toxic toward cancer cells (human promyelocytic leukemia (HL-60), $IC_{50} = 9 \mu M$, and human glioblastoma-astrocytoma (U373), $IC_{50} = 25 \mu M$), but not toxic (up to $100 \mu M$) toward representative nonmalignant cells (fibroblasts).

INTRODUCTION

Cancer is a group of diseases which is caused by abnormalities in the genetic material of the transformed cells. One of the most successful methods of cancer treatment is chemotherapy with cytotoxic drugs that is often used in combination with surgery and radiotherapy. Cisplatin, oxaliplatin,¹ and 5-fluorouracil² are representative examples of practically important anticancer drugs. Though these agents target rapidly dividing cells, their cell specificity is usually low. For example, healthy tissues with a quick replacement rate (e.g., intestinal lining) and rapidly dividing normal cells (e.g., cells of the hematopoietic system) are especially strongly affected.

The tumor microenvironment is different from that of normal tissues. For example, most cancer cells both in isolated form and in tissue exhibit enhanced reactive oxygen species (ROS) production.³ ROS include 1O_2 , O_2^- , HO^\bullet , and H_2O_2 . As a consequence, they function at higher concentrations of ROS. For example, the maximal intracellular concentration of H_2O_2 ($[H_2O_2]_{in}$) in Jurkat T-cells was determined to be $7 \mu M$.^{3d} Some cancer cells are known to resist 0.1–10 mM extracellular H_2O_2 ($[H_2O_2]_{out}$).^{3e,f} Since $[H_2O_2]_{in}$ was found to be 7–10-fold below $[H_2O_2]_{out}$,^{3d} one may estimate that $[H_2O_2]_{in}$ in some cancer cells may reach 10–100 μM . In contrast, $[H_2O_2]_{in}$ in normal cells varies between 0.001 and 0.7 μM , while $[H_2O_2]_{in} = 1 \mu M$ is already toxic.^{3g} Since they function with a heightened basal level of ROS, cancer cells are more vulnerable to oxidative stress than healthy cells.³ Therefore, exogenous compounds inducing production of ROS or other radicals can potentially be used as anticancer drugs. Examples of such

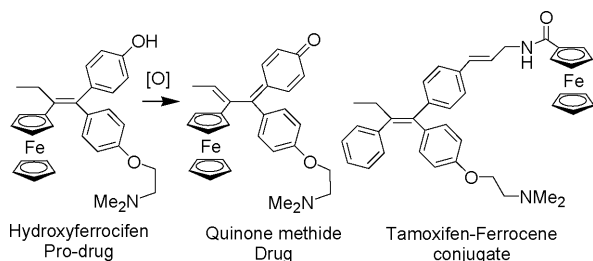
compounds are arsenic trioxide,⁴ buthionine sulfoximine,⁵ procarbazine,^{5b} β -phenylethyl isothiocyanate,⁶ NO-ASA,⁷ metexafin gadolinium,^{5b,8} ferrocenium ion containing salts,⁹ and $[(\eta^6\text{-arene})Ru(\text{azpy})]^{+}$ complexes.¹⁰ Unfortunately, these ROS regulating drugs not only kill cancer cells, but also increase the ROS amount in normal cells. Though the increased ROS does not kill normal cells, it can stimulate their transformation, thus potentially inducing secondary tumors.¹¹

Prodrugs, which are converted to toxic species at cancer-specific conditions (e.g., high ROS), potentially lack this dangerous side effect. For example, Jaouen and co-workers have developed an anticancer drug, hydroxyferrocifen, a ferrocenyl analogue of 4-hydroxytamoxifen (Scheme 1).¹² This compound is converted in cells into toxic quinone methide (QM),^{7,13} which alkylates glutathione (GSH), thus inhibiting the antioxidative system of cells. The ferrocene fragment in this prodrug facilitates formation of the quinone methide rather than acts itself as a catalyst of ROS generation. In particular, Salganik and co-workers have observed that ferrocifen analogues, which are unable to form quinone methides (tamoxifen–ferrocene, Scheme 1), do not exhibit high cytotoxicity.¹⁴ Examples are known where the ferrocene-containing drugs act by alternative mechanisms, neither ROS nor *p*-quinone methide related. In particular, Jaouen and co-workers have prepared ferrocenes carrying two aminoalkyl chains.¹⁵ The authors suggested that antiproliferative properties

Received: November 7, 2011

Published: December 19, 2011

Scheme 1. Structures of Hydroxyferrocifen and Its Active Metabolite (Quinone Methide)¹² and a Conjugate of Tamoxifen with Ferrocene¹⁴



of these compounds on hormone-independent MDA-MB-231 cells can be explained by their ability to bind Zn^{2+} . Here, the ferrocene fragment seems to play a purely structural role.

Herein we report on novel ferrocenes, which, as well as hydroxyferrocifen, are activated in cancer cells by oxidation with generation of quinone methide species. In addition to that, an efficient catalyst for ROS production is formed during the activation process (Figure 1). We demonstrated that these

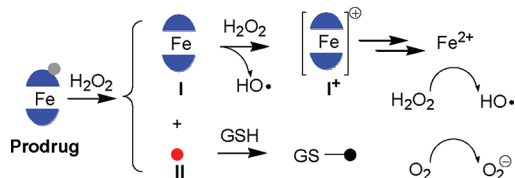


Figure 1. Concept of an anticancer prodrug activated by H_2O_2 : blue half-circles, ligands binding iron; gray circle, a H_2O_2 -sensitive protecting group. The prodrug is converted in cancer cells (high ROS) into I (aminoferrocene) and II (*p*-quinone methide). Compound II alkylates GSH, and I is converted to the toxic ferrocenium derivative (I^+), which can be degraded to free iron ions. Both I^+ and iron ions generate ROS catalytically.

organometallic complexes exhibit anticancer activity in cellular assays and target cancer cells selectively over normal cells. In particular, we tested representative cancer cell lines (non-adherent, human promyelocytic leukemia (HL-60), and adherent, human glioblastoma-astrocytoma (U373)) and non-malignant cells (fibroblasts). To the best of our knowledge, they are the first prodrugs, which are able to simultaneously inhibit the antioxidative cellular system and to induce catalytic generation of ROS.

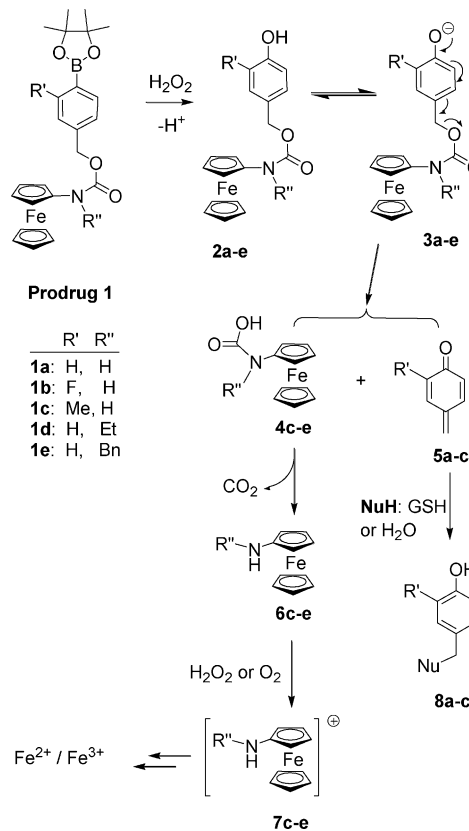
Cytotoxic Ru(II) complexes $[(\eta^6\text{-arene})Ru(\text{azpy})I]^+$ reported by the group of Sadler also act by the dual mechanism.¹⁰ In particular, they first oxidize GSH to GSSG. The oxidant in this case is the 2-(phenylazo)pyridine ligand coordinated to Ru. Then the recovery of the initial complexes in the presence of O_2 occurs by generation of H_2O_2 . In contrast to our metal complexes, these Ru(II) complexes are not prodrugs. Therefore, they can also potentially affect normal cells. Moreover, the oxidized product (GSSG) can be recovered by intracellular reductases, which should diminish the effect of the drug.

Among other prodrugs activated at disease-specific conditions, pro-antioxidants have also been described. Examples include metal binding ligands and matrix metalloprotease (MMP) inhibitors, which are triggered in the presence of H_2O_2 ,¹⁶ specific enzymes,¹⁷ and protons.¹⁸

RESULTS AND DISCUSSION

Concept. The structure of prodrug 1 is shown in Scheme 2. It is a derivative of aminoferrocene, which is linked to the

Scheme 2. Structure of Prodrug 1 and Its Activation in the Presence of Hydrogen Peroxide with Formation of Cytotoxic *p*-Quinone Methide 5, Ferrocenium Ions 7, and Iron Ions



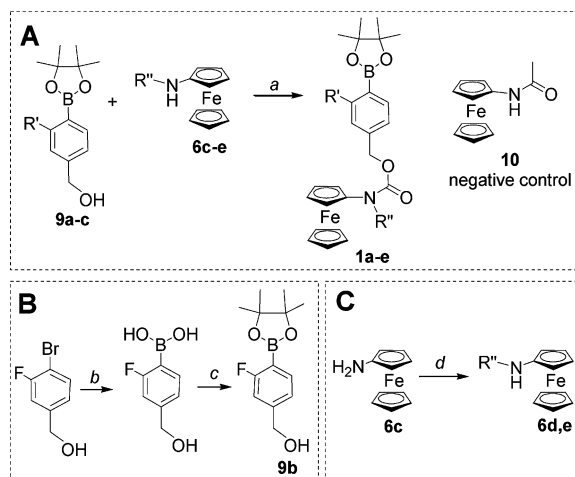
pinacol ester of 4-(hydroxymethyl)phenylboronic acid via a carbamate linker. We envisioned that this prodrug would be activated at cancer-specific conditions (high ROS, e.g., H_2O_2) in accordance with the mechanism outlined in Scheme 2. In particular, the B–C bond is first cleaved in the presence of hydrogen peroxide with formation of phenol 2. The latter compound exists in aqueous solution in equilibrium with phenolate 3 ($pK_a \approx 9$), which undergoes spontaneous 1,6-elimination¹⁵ with formation of compound 4 and *p*-quinone methide 5. Compound 4 is unstable. In aqueous solution it is cleaved, forming CO_2 and aminoferrocene 6. This sequence of the cleavage reactions shifts the phenol \rightarrow phenolate equilibrium to the right until all phenol is used up. Both compounds 5 and 6 are expected to be cytotoxic and act in a concerted fashion. In particular, aminoferrocene 6 is first oxidized by H_2O_2 or O_2 , forming aminoferrocenium cation 7 and either hydroxyl radicals (HO^\bullet) or superoxide anion radical ($O_2^{\bullet-}$). 7 is further decomposed in water with formation of iron ions. The latter ions can also catalyze generation of toxic ROS from less reactive H_2O_2 or O_2 .¹⁹ Furthermore, *p*-quinone methide 5 reacts with ROS scavengers such as GSH with formation of alkylated products 8,¹³ which are not efficient ROS scavengers. It has been previously demonstrated that *p*-quinone methide releasing compounds can affect cancer cells. For example, Wijtmans and co-workers have described NO-ASA drug, which is activated in the presence of esterases with

generation of *p*-quinone methide.⁷ NO-ASA was found to be toxic toward SW480 cells (human colon adenocarcinoma, IC₅₀ = 85 μM) and HT29 cells (human colon adenocarcinoma, IC₅₀ = 3–7 μM).²⁰ In contrast to a monofunctional drug such as NO-ASA, prodrug **1** not only inhibits the antioxidant system of the cancer cell by generating *p*-quinone methide **5**, but also generates reactive ROS catalytically in the presence of the iron complexes (**6**, **7**, and iron ions). These processes are expected to act synergistically.

We prepared a series of prodrugs **1** with different substituents R' and R'' (Scheme 2). These substituents were expected to modulate cell-membrane permeability of the prodrugs and their reactivity toward H₂O₂.

Synthesis of Prodrugs. Starting materials **9a–c** and **6c–e** were required for synthesis of compounds **1a–e** (Scheme 3).

Scheme 3. Synthesis of the Prodrugs (A) and the Corresponding Starting Materials, Which Were Not Reported Before (B, C)^a



^aReagents and conditions: (a) triphosgene, toluene, 120 °C; (b) (1) NHMe₂, BuLi, -78 °C; (2) B(OiPr)₃, -78 °C; (3) aqueous NaOH; (c) pinacol, 22 °C; (d) R''C(=O)H, Na[B(CN)H₃].

9a was purchased from commercial sources, **9c** was prepared by esterification of 4-(hydroxymethyl)-3-methylphenylboronic acid with pinacol, and **9b** was obtained in accordance with Scheme 3B. In particular, the boronic acid residue was first introduced in place of the bromide in 4-bromo-3-fluorobenzyl alcohol. The same protocol was applied earlier by the group of Armstrong to prepare similar arylboronic acids.²¹ The resulting 4-(hydroxymethyl)-3-fluorophenylboronic acid was esterified with pinacol to obtain **9b**. Aminoferrocene **6c** was prepared according to the protocol reported by the group of Heinze.²² Its alkylated derivatives **6d** and **6e** were obtained by reductive amination of **6c** in the presence of correspondingly acetaldehyde and benzaldehyde (Scheme 3B).

Prodrugs **1** (Scheme 3) were synthesized by coupling aminoferrocenes **6c–e** with pinacol esters of 4-(hydroxymethyl)phenylboronic acids **9a–c** in the presence of triphosgene. Yields of the isolated products were in the range of 5–71%. The prodrugs based on the unsubstituted aminoferrocene (R' = H, **1a–c**) were obtained with higher yields (24–71%) than those with R' ≠ H (**1d–e**, <20%). The latter fact is explained by the lower reactivity of the substituted aminoferrocenes with triphosgene.

Transformations of the Prodrugs in the Presence of Hydrogen Peroxide. We studied the cleavage/activation of the prodrugs (0.9 mM) in the presence of hydrogen peroxide (9 mM) by using electrospray ionization (ESI) mass spectrometry. The data for two representative compounds, **1a** and **1e**, are shown in Figure 2. The experiments were

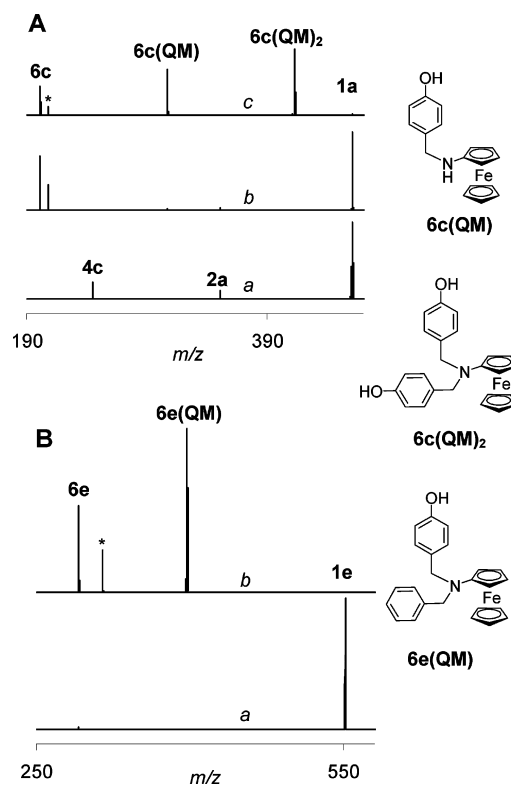


Figure 2. ESI mass spectra of mixtures consisting of hydrogen peroxide (9 mM), triethylamine (0.9 mM), and either prodrug **1a** (A) or prodrug **1e** (B) (concentration of the prodrugs 0.9 mM) in CH₃CN/water (10/1.1, v/v) solution. After addition of H₂O₂ to the mixtures and their incubation for the specific time, the mass spectra were acquired: (A) incubation times are 2 min (a), 5 min (b), and 10 min (c); (B) incubation times are 2 min (a) and 10 min (b). The labeling scheme used is explained in Scheme 2; nonassigned peaks are labeled with an asterisk.

conducted in CH₃CN/water (10/1.1, v/v) solvent mixtures whose pH was adjusted to 7 by addition of NEt₃. The peak corresponding to the product of the B–C bond cleavage in prodrug **1a** (**2a**) was observed already 2 min after addition of H₂O₂ (trace a, Figure 2A). As expected, the intensity of this peak is decreased with increasing incubation time (traces b and c). The peak corresponding to the product of phenolate decomposition (aminoferrocene **6c**) could be detected after 5 min of incubation (trace b). Another product of the latter reaction should be *p*-quinone methide **5**. This compound was observed neither in positive nor in negative detection mode in the spectra of the corresponding mixtures. However, we could detect the product of scavenging of **5** by water by using thin-layer chromatography (TLC) and the corresponding reference compound 4-(hydroxymethyl)phenol (Figure S13, Supporting Information). Moreover, we observed that both [N-(4-hydroxybenzyl)amino]ferrocene (**6c(QM)**) and [N,N-bis(4-hydroxybenzyl)amino]ferrocene (**6c(QM)₂**) were formed in prodrug **1**/H₂O₂ mixtures after 10 min of incubation, which

confirms the formation of electrophilic *p*-quinone methide at these conditions. These products were not formed at lower concentrations of the prodrugs ($\leq 100 \mu\text{M}$, data not shown). Since experiments with cells were conducted with prodrugs at $\leq 100 \mu\text{M}$, one does not expect that $6c(\text{QM})_x$ ($x = 1, 2$) adducts will be generated in cells. In accordance with literature reports,¹³ in cells, **5** would rather alkylate more nucleophilic glutathione, which is present in high concentrations, 5–10 mM. Prodrug **1e** is degraded in the presence of hydrogen peroxide similarly to **1a** (Figure 2B). In particular, after 10 min of incubation with H_2O_2 , compound **1e** is fully decomposed with formation of (*N*-benzylamino)ferrocene (**6e**) and its adduct with *p*-quinone methide (**6e(QM)**).

Iron Release from Prodrugs 1a–e. The fate of aminoferrocenes released from the prodrugs in the presence of H_2O_2 was studied next by using ESI mass spectrometry and UV–vis spectroscopy. In particular, we observed that in the mass spectra of mixtures of **6c** (0.9 mM) and H_2O_2 (90 mM) the peak corresponding to **6c** disappeared after 10 min of incubation, whereas two new peaks appeared, at 162 *m/z*, which corresponds to bis(aminocyclopentadiene) ($(\text{H}_2\text{N-CpH})_2$), and at 132 *m/z*, which corresponds to dicyclopentadiene ($(\text{CpH})_2$; Figure 3). These spectral changes indicate that

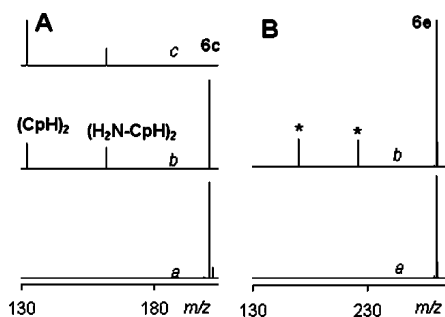


Figure 3. ESI mass spectra of mixtures consisting of hydrogen peroxide (90 mM), triethylamine (0.9 mM), and either **6c** (A) or **6e** (B) (concentration 0.9 mM) in $\text{CH}_3\text{CN}/\text{water}$ (10/1.1, v/v) solution. After addition of H_2O_2 to the mixtures and their incubation for the specific time, the mass spectra were acquired: (A) incubation times are 2 min (a), 5 min (b), and 10 min (c); (B) incubation times are 2 min (a) and 20 min (b). $(\text{CpH})_2$ = dicyclopentadiene, and $(\text{H}_2\text{N-CpH})_2$ = bis(aminocyclopentadiene). Nonassigned peaks are labeled with an asterisk.

6c is decomposed in the presence of H_2O_2 with release of the ligands. Another product obtained in this reaction should be iron ions. Thus, H_2O_2 -induced decomposition of prodrugs **1a–c** does not stop at the stage of aminoferrocene **6c**. We confirmed this conclusion by detecting iron ions in mixtures of prodrugs **1a–c** and H_2O_2 by using the chromogenic reaction with 2,2'-bipyridine (bipy). This assay is based on the formation of red $[\text{Fe}(\text{bipy})_3]^{2+}$ complex in the presence of iron(II) ions (Figure 4A,B). For example, we observed that H_2O_2 (1 mM) induced conversion of 95% of prodrug **1a**, 92% of **1b**, and 74% of **1c** (0.1 mM) into iron ions within 100 min. We explain the lower conversion of **1c** by the +I effect of the 2-methyl group (*R'*, Scheme 2). In particular, the electron donor group *R'* disfavors formation of the phenolate **3c**, leading to lowering of the yield of iron ions released from prodrug **1c**. We observed that the amount of iron released from the prodrugs was proportional to the reaction time and the concentration of hydrogen peroxide (Figure 4C,D). As expected, a negative

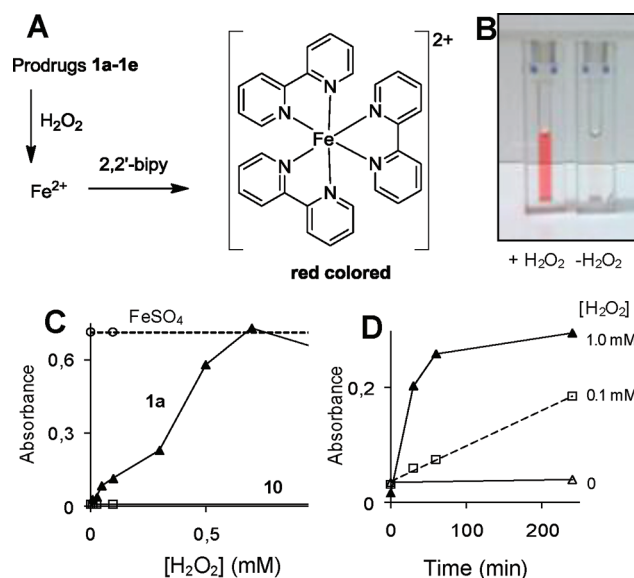
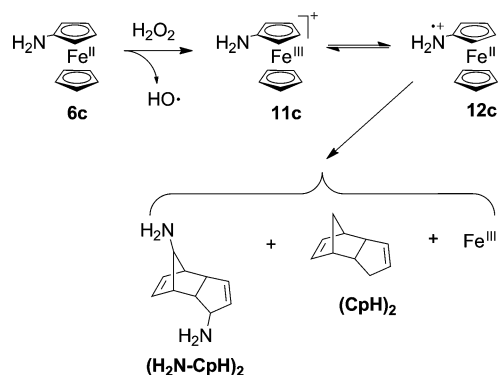


Figure 4. (A) Reaction scheme used for detection of iron ions released from prodrugs **1a–e** in the presence of H_2O_2 . (B) Prodrug **1a** (0.1 mM) dissolved in MOPS buffer (100 mM, pH 7.5) and treated (left cuvette) or not treated (right cuvette) with H_2O_2 (10 mM) for 100 min and then with sodium dithionite (20 mM) and 2,2'-bipyridine (300 μM). (C) Absorbance at 519 nm of mixtures containing iron complexes indicated on the plot (100 μM) dissolved in MOPS buffer (100 mM, pH 7.5) and treated with varying H_2O_2 concentrations for 100 min. Before the absorbance measurement the mixture was treated with sodium dithionite (20 mM) and 2,2'-bipyridine (300 μM). (D) Kinetics of iron release from prodrug **1a** in the absence of H_2O_2 and presence of H_2O_2 (0.1 and 1.0 mM). All conditions are the same as described for (C).

control, (*N*-acetylamino)ferrocene (**10**), which does not contain the cleavable group, was stable in the presence of H_2O_2 .

It has previously been known that aminoferrocene **6c** is not stable under oxidative conditions.²³ However, neither the rate nor the mechanism of its decomposition in aqueous solution has been reported yet. On the basis of our data, we suggested the mechanism of oxidative decomposition of **6c**, which is outlined in Scheme 4. In the first step, an $18e^-$ iron(II)

Scheme 4. Possible Mechanism of Decomposition of Aminoferrocene **6c** under Oxidative Conditions



complex, **6c**, is oxidized with formation of a $17e^-$ iron(III) complex, **11c**, and a $18e^-$ radical iron(II) complex, **12c**. The latter compound is expected to be unstable due to its electron deficiency. It is decomposed with formation of the ligands and

iron ions. Among the prodrugs based on alkylated aminoferrocenes (**1d**, **1e**), only **1d** generates in the presence of H_2O_2 (1 mM) iron ions in amounts comparable to those released from prodrugs **1a–c** at the same conditions, 72% in 100 min (Table 1). In contrast, the H_2O_2 -induced degradation of **1e** is

Table 1. Efficacy of Release of Iron Ions and ROS Generation in Vitro from the Prodrugs and Control Compounds in the Presence of H_2O_2

entry	iron complex ^a	efficacy of iron release ^b (%)	efficacy of ROS generation ^c (%)
1	FeSO_4	100	100
2	10	0	4
3	1a	95	56
4	1b	92	50
5	1c	74	52
6	1d	72	50
7	1e	9	24 (53) ^d

^aStructures of prodrugs **1a–e** are given in Scheme 2. Compound **10** is a negative control, (*N*-acetylamino)ferrocene. ^bIron release efficacy = $(A_{519\text{ nm}}(\text{prodrug}) - A_{519\text{ nm}}(\text{buffer})) / (A_{519\text{ nm}}(\text{FeSO}_4) - A_{519\text{ nm}}(\text{buffer}))$, where $A_{519\text{ nm}}(\text{prodrug})$ is the absorbance at 519 nm of a prodrug (100 μM) solution in MOPS buffer (100 mM, pH 7.5), which was treated first with H_2O_2 (1 mM) for 100 min and then with $\text{Na}_2\text{S}_2\text{O}_4$ (20 mM) and 2,2'-bipyridine (300 μM) and $A_{519\text{ nm}}(\text{buffer})$ and $A_{519\text{ nm}}(\text{FeSO}_4)$ are the absorbances at 519 nm of the MOPS buffer and iron sulfate (100 μM) dissolved in this buffer treated similarly to the prodrug. The experiments were conducted at least three times. The standard deviation is not higher than 11% of the values given in the table. ^cEfficacy of ROS release = $(F(\text{prodrug}) - F_0) / (F(\text{FeSO}_4) - F_0)$, where $F(\text{prodrug})$ is the emission at 531 nm ($\lambda_{\text{ex}} = 501\text{ nm}$) of a solution containing MOPS buffer (100 mM, pH 7.5), EDTA (10 mM), glutathione (5 mM), 2',7'-dichlorofluorescein (10 μM), and H_2O_2 (10 mM), which was incubated with a prodrug (100 μM) for 17 min, $F(\text{FeSO}_4)$ is the emission of a mixture containing FeSO_4 in place of the prodrug, and F_0 is the emission of a mixture containing no iron complex. The experiments were conducted at least three times. The standard deviation is not higher than 10% of the values given in the table. ^dIncubation time 37 min.

practically stopped at the stage of aminoferrocene **6e**: **1e** generates only 9% of iron ions in the presence of 1 mM H_2O_2 within 100 min. This conclusion was corroborated by the mass spectrometric study (Figure 3). In particular, the intense peak of **6e** (0.9 mM) was observed in the mass spectra during at least 20 min of its incubation with H_2O_2 (90 mM). For comparison, **6a** was not detectable in the mass spectra already after 10 min of its incubation with the same concentration of H_2O_2 (compare trace c in Figure 3A with trace b in Figure 3B).

On the basis of the above suggested mechanism of the oxidative degradation of aminoferrocene (Scheme 4), the higher stability of *N*-benzyl-substituted **6e** than unsubstituted **6c** or *N*-ethyl-substituted **6d** can be explained by the stronger electron acceptor effect (–I) of the benzyl group in comparison to the proton or the ethyl substituent (R'' in Scheme 2). We estimated the inductive effects by comparing the basicities of anilines, which can be considered as analogues of aminoferrocenes ($\text{p}K_{\text{a}}$): PhNHEt (5.12), PhNH_2 (4.63), and PhNHCH_2Ph (3.89).²⁴ The stronger electron acceptor effect of the Bn group leads to the destabilization of the radical cation **12c**. Consequently, less of this ion is formed and less iron ions are released upon its decomposition. The detailed theoretical study of the reaction of oxidative cleavage of aminoferrocenes

6c–e is currently under way and will be published separately in due course.

Amino substituents at the ferrocene periphery are strongly activating groups for ferrocene oxidation with formation of ferrocenium ions (Fc^+). For example, the oxidation potential of aminoferrocene **6c** was found to be 0.37 V more negative than that of ferrocene.²⁵ We observed that the oxidizing potential of (*N*-benzylamino)ferrocene (**6e**) was also substantially more negative (0.34 V) than that of ferrocene. Correspondingly, one could expect that Fc^+ species will be formed from compound **6e** in the presence of oxidants such as H_2O_2 and O_2 . According to the data reported by Sohn et al.,²⁶ formation of Fc^+ ions from ferrocenes correlates with the increased light absorption in the region between 250 and 350 nm. In this spectral region, ferrocene derivatives exhibit intense charge transfer transitions whereas ferrocenes have only weak transitions. We observed that absorbance at 300 nm of solutions of prodrug **1e** is strongly increased upon addition of H_2O_2 . The increase was substantially weaker in the presence of **1c** and **1d** (Figure 5).

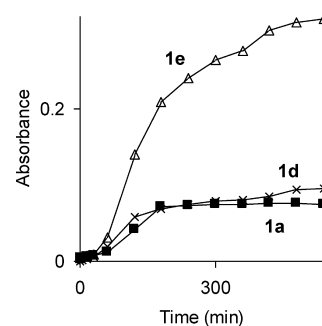


Figure 5. Iron complexes (100 μM) were dissolved in dimethylformamide (100 μL), and concentrated H_2O_2 solution (30% in water, 1 μL) was added: the final H_2O_2 concentration was 9.8 mM. Light absorbance at 300 nm was monitored as a function of time.

Thus, we can conclude that after formation of **6e** from the prodrug **1e** ($\text{R}'' = \text{Bn}$) and H_2O_2 the former compound is further converted to ferrocenium species [**6e**]⁺.

Not only hydrogen peroxide, but also other naturally occurring reactive oxygen species can potentially induce activation of our prodrugs. In particular, we have studied the stability of the representative prodrug **1a** in the presence of hydroxyl radicals (HO^\bullet), singlet oxygen ($^1\text{O}_2$), and superoxide anion radical (O_2^- ; Figure S14, Supporting Information). We observed that hydroxyl radicals activated **1a** more efficiently than hydrogen peroxide, whereas the reactivity of singlet oxygen and superoxide anion radical was substantially lower.

Generation of Reactive Oxygen Species in the Presence of Prodrugs 1a–e. In accordance with the data described above, prodrugs **1a–d** are decomposed in the presence of H_2O_2 with formation of iron ions whereas prodrug **1e** generates Fc^+ species. All these products can act as catalysts of conversion of less reactive H_2O_2 into highly reactive hydroxyl radicals (HO^\bullet).^{9,19} We studied the reaction of generation of hydroxyl radicals in mixtures containing prodrugs and H_2O_2 by using a fluorogenic 2',7'-dichlorofluorescein probe. As a positive control we took FeSO_4 salt and as a negative control (*N*-acetylamino)ferrocene (**10**), which was found to be stable toward H_2O_2 (Figure 4). The kinetics of HO^\bullet generation in the presence of positive and negative controls, as well as of a representative prodrug **1a**, are shown in Figure 6.

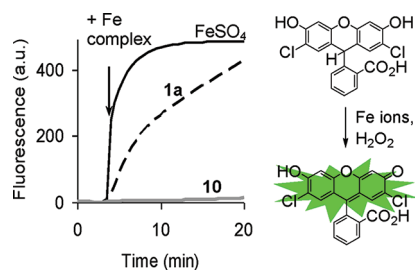


Figure 6. Monitoring changes of the fluorescence intensity ($\lambda_{\text{ex}} = 501$ nm, $\lambda_{\text{em}} = 531$ nm) of solutions containing 2',7'-dichlorofluorescein (10 μM), iron complex (100 μM), MOPS buffer (100 mM, pH 7.5), N,N,N',N' -ethylenediaminetetraacetic acid (EDTA; 10 mM), glutathione (5 mM), and H_2O_2 (10 mM). Iron complexes (100 μM) were added at the time point indicated by an arrow. The fluorescence is increased due to HO^\bullet -induced oxidation of nonfluorescent 2',7'-dichlorofluorescein to fluorescent 2',7'-dichlorofluorescein.

The rate of this reaction in the presence of **1a** is increased with time (Figure 7), which indicates that the reaction is

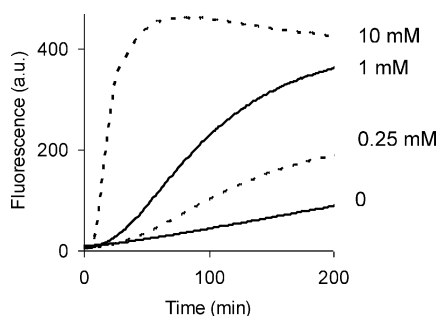


Figure 7. Monitoring changes of the fluorescence intensity ($\lambda_{\text{ex}} = 501$ nm, $\lambda_{\text{em}} = 531$ nm) of solutions containing prodrug **1a** (100 μM), 2',7'-dichlorofluorescein (100 μM), MOPS buffer (100 mM, pH 7.5), EDTA (10 mM), glutathione (5 mM), and variable amounts of H_2O_2 (concentrations are shown on the plot).

autocatalytic.²⁷ This is caused by formation of a highly active catalyst (iron ions) as a product.

The efficacy of HO^\bullet generation was determined for all prepared prodrugs 17 min after the addition of the iron complex to a mixture of H_2O_2 and 2',7'-dichlorofluorescein (Table 1). As a reference (100%) we used the ROS amount released in the presence of FeSO_4 . We observed that the efficiency of ROS generation by prodrugs **1a–d** correlates with the efficiency of iron release from these compounds (Table 1). It is noteworthy that, though prodrug **1e** releases an 8.2–10.6-fold lower amount of iron ions than **1a–d**, it generates only ~2 times less hydroxyl radicals (24%) than the corresponding prodrugs (Table 1). These data indicate that both ferrocenium ions released from **1e** as a major product and iron ions (minor product) act in this case as catalysts of ROS generation. Though prodrug **1e** generates less ROS than other prodrugs within 17 min, when the reaction is allowed to proceed longer, the amount of ROS released in the presence of this compound is increased to the level of that of prodrugs **1a–d**, 53% (in 37 min, Table 1). The lower reactivity can be considered as an advantage of **1e** over other studied prodrugs, since this property may result in its higher selectivity toward cancer cells.

Cytotoxicity of Prodrugs 1a–e. The natural abundance of boron in cells is rather low. Therefore, we could determine the cell membrane permeability of prodrugs **1a–e** by

monitoring the boron concentration in cells before and after their incubation with the prodrugs. Boron was detected by using a curcumin probe in accordance with a protocol described elsewhere (Table 2).²⁸

Table 2. Cytotoxicity, Cellular Membrane Permeability, and ROS Generation Efficiency of Prodrugs **1a–e** and Controls

entry	Fe complex	IC_{50}^a (μM)	membrane permeability ^b	efficacy of ROS generation in cells ^c
1	$\text{Fe}(8\text{-HQ})_2^d$	3 ± 1		
2	10	>200		1.1 ± 0.2
3	1a	52 ± 3	1.0 ± 0.2	17.5 ± 1.4
4	1b	55 ± 4	0.3 ± 0.1	12.3 ± 0.8 (41) ^e
5	1c	40 ± 3	1.3 ± 0.2	20.0 ± 1.1 (15.4)
6	1d	24 ± 2	3.1 ± 0.3	25.7 ± 2.1 (8.3)
7	1e	9 ± 2	1.8 ± 0.3	28.8 ± 2.3 (16)
8	6e	>200		

^aHL-60 cells were incubated with iron complexes over 48 h, and their viability was determined by using the MTT assay (MTT = 3-(4,5-dimethylthiazol-2-yl)-2,5-diphenyltetrazolium bromide). ^bThe cell membrane permeability of prodrugs **1a–e** was determined by detecting the boron concentration in cells after their incubation with the prodrugs. **1a** was used as a reference: its permeability was set to be 1, and its absolute amount in cells corresponds to 4.4 fmol/cell. ^cROS generation in cells was monitored by using 2',7'-dichlorofluorescein diacetate. Efficacy = $F(\text{prodrug})/F_0$, where $F(\text{prodrug})$ is the mean fluorescence intensity of cells incubated with a prodrug and F_0 is the mean fluorescence intensity of cells which were not treated with any iron complex. The prodrug concentration is 100 μM . ^d $\text{Fe}(8\text{-HQ})_2$ is a positive control which was used to load cells with iron ions; this complex is formed from 1 equiv of FeCl_3 and 2 equiv of 8-hydroxyquinoline. ^eIn parentheses is given the relative ROS generation efficacy corrected for the membrane permeability of prodrugs, which is equal to $[F(\text{prodrug})/F_0]/(\text{relative membrane permeability})$.

The permeability of prodrug **1a** ($R' = R'' = \text{H}$) was taken as a reference. We observed that, relative to this compound, a more polar **1b** ($R' = \text{F}$, $R'' = \text{H}$) is ~3 times less permeable (entry 4) whereas less polar **1c** ($R' = \text{CH}_3$, $R'' = \text{H}$), **1d** ($R' = \text{H}$, $R'' = \text{CH}_2\text{CH}_3$), and **1e** ($R' = \text{H}$, $R'' = \text{CH}_2\text{Ph}$) are 1.3–3.1-fold more permeable (entries 5–7). The cell loading with the reference compound **1a** corresponds to 4.4 fmol/cell.

Next we studied the cytotoxicity of the prodrugs and control compounds on the human promyelocytic leukemia cell line (HL-60; Table 2). In these experiments an iron(III) complex with 8-hydroxyquinoline ($\text{Fe}(8\text{-HQ})_2$) was applied as a positive control. This coordination compound permeates the cell membrane substantially more quickly than simple iron salts do, which allows loading the cells with iron ions in a reproducible fashion.²⁹ We observed that $\text{Fe}(8\text{-HQ})_2$ is highly cytotoxic, $\text{IC}_{50} = 3 \pm 1$ μM (entry 1). In contrast, stable ferrocene complex **10** (negative control) is not toxic at all, $\text{IC}_{50} > 200$ μM (entry 2). This confirms that simple ferrocenes are not efficient catalysts of ROS generation in cells. The cytotoxicity of prodrugs **1a–e** is intermediate between those of positive and negative controls (entries 3–7, Table 2). The most efficient complex in this series is prodrug **1e**, whose $\text{IC}_{50} = 9 \pm 2$ μM (entry 7). It is the only compound which releases ferrocenium species rather than iron ions in the presence of hydrogen peroxide (see the discussion above). These data indicate that in cells Fc^+ is more cytotoxic than iron ions. This is a surprising fact, since in vitro iron ions are more potent catalysts of ROS generation than Fc^+ ions (Table 1). We

suggest that the reactivity is reversed due to the ability of cells to neutralize iron overload via efficient natural, biochemical mechanisms. In contrast, Fc^+ is not a natural compound. Therefore, its metabolism is probably substantially slower. Consequently, the lifetime of Fc^+ in the cell should be longer. We observed that the cytotoxicity of all iron releasing prodrugs **1a–d** correlates well with their membrane permeability (Figure

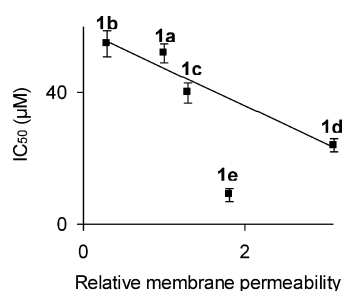


Figure 8. Correlation of the cytotoxicity of prodrugs **1a–e** and their cell membrane permeabilities.

8). In contrast, the properties of prodrug **1e** strongly deviate from this correlation. These data also support our conclusion that complexes **1a–d** and **1e** release different active species in cells.

According to the data discussed above, prodrug **1e** acts in the following fashion: it permeates the cellular membrane, is converted into toxic *p*-quinone methide (**5a**) and intermediate **6e**, and finally **6e** is oxidized with formation of another toxic component, $[\text{6e}]^+$ (Scheme 2). Therefore, providing it reaches the intracellular space, intermediate **6e** should also exhibit some cytotoxicity due to the generation of toxic ferrocenium species. Interestingly, we observed that **6e** itself is not cytotoxic at all (Table 2). This fact may indicate that **6e** is not cell membrane permeable. However, simple, uncharged ferrocenes usually permeate the cellular membrane well. We explain these data in the following way. Since compound **6e** has an unusually low oxidation potential (-0.34 V versus ferrocene), it is easily oxidized in air with formation of $[\text{6e}]^+$. Indeed, we observed that already 1 h after its dissolution in the medium saturated with air, compound **6e** could not be detected by thin-layer chromatography. In contrast, a colored, low-mobility spot was detected which may correspond to ferrocenium species. The ferrocenium complex $[\text{6e}]^+$ is charged and can have low membrane permeability. Thus, in contrast to **1e**, compound **6e** is not applicable as a prodrug.

Furthermore, we tested the cytotoxicity of our most active prodrug **1e** toward other cell types: human glioblastoma-astrocytoma cells (U373) and fibroblasts (Figure 9). The former ones are malignant cells, whereas the latter ones are normal (nonmalignant) cells. We observed that as well as HL-60 cells U373 cells were sensitive to prodrug **1e** ($\text{IC}_{50} = 25 \pm 2$ µM) whereas normal cells (fibroblasts) turned out to be resistant at a concentration of the prodrug of up to 100 µM (Figure 9). In particular, after incubation of fibroblasts for 48 h with **1e** (100 µM), 78% of the cells (relative to the control cells, which were incubated in the medium only) remained viable. In contrast, only 4% of the HL-60 cells and 0% of the U373 cells incubated with **1e** (100 µM) for 48 h remained viable. These data indicate that **1e** is substantially more toxic to malignant cells ($\text{IC}_{50} = 9–25$ µM) than to nonmalignant fibroblasts ($\text{IC}_{50} > 100$ µM).

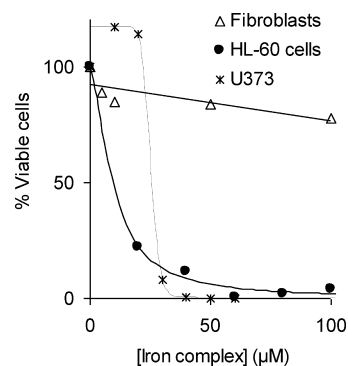


Figure 9. Cytotoxicity of prodrug **1e** toward cancerous and noncancerous cells: human promyelocytic leukemia (HL-60), human glioblastoma-astrocytoma (U373), and fibroblasts.

By using 2',7'-dichlorofluorescein diacetate as an intracellular probe, we observed that the incubation of HL-60 cells with the prodrugs **1a–e** (100 µM) for 5 h leads to a significant increase of the intracellular concentration of ROS (Table 2). In contrast, stable ferrocene derivative **10** does not affect the intracellular concentration of ROS at the same conditions. Interestingly, the ROS amount present in normal cells (fibroblasts) was found to be >10-fold lower than that in cancer cells (HL-60, Figure S15, Supporting Information), which is in agreement with the low toxicity of prodrug **1e** toward normal cells (Figure 9). The cytotoxicity of the prodrugs correlates with the efficacy of ROS generation in cells loaded with these prodrugs (Figure 10). These data confirm the mechanism of cytotoxicity of the prodrugs, which is outlined in Figure 1 and Scheme 2.

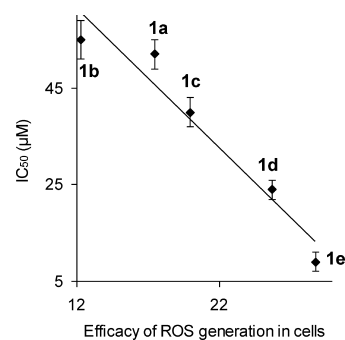


Figure 10. Correlation of the cytotoxicity of the prodrugs **1a–e** and the efficacy of ROS generation in cells loaded with these prodrugs. The data used to plot this graph and the experimental conditions for determination of IC_{50} values and efficacies of the ROS generation are presented in Table 2 and its footnotes.

Since the medium is known to scavenge excess ROS, which is released by cancer cells, the ROS concentration in cultivated cells is expected to be lower than that in the same cells in vivo. To model the microenvironment of cancer cells in vivo, we preincubated the cells with nontoxic H_2O_2 concentrations for 1 h (Supporting Information). We found that cells prepared in such a way were 1.4-fold (U373) to 3-fold (HL-60) more sensitive to the representative prodrug **1a** than the untreated cells.

Interestingly, HL-60 cells overexpressing catalase (HL-60cat) exhibit H_2O_2 -independent sensitivity to prodrug **1a**. These data additionally confirm that H_2O_2 indeed acts as an intracellular trigger of the activity of the prodrugs.

CONCLUSIONS

We prepared five novel aminoferrocene-based prodrugs which are protected with a 4-[(carbonyloxy)methyl]phenylboronic acid pinacol ester residue. We demonstrated that four of these prodrugs are activated at cancer-specific conditions (high concentration of reactive oxygen species) with formation of toxic *p*-quinone methide and iron ions. In contrast, one of the prodrugs (4-[[[*N*-ferrocenyl-*N*-benzylamino]carbonyl]oxy]methyl]phenylboronic acid pinacol ester, **1e**) is activated at the same conditions with formation of *p*-quinone methide and (benzylamino)ferrocenium ($[\text{6e}]^+$) ions. The released products act in a concerted fashion. In particular, *p*-quinone methide alkylates glutathione and inhibits the antioxidative system of the cell, whereas iron or ferrocenium ions induce catalytic generation of highly reactive ROS (hydroxyl radicals). The activation reaction proceeds autocatalytically, which leads to generation of large quantities of ROS in cancer cells. We observed that among the studied compounds **1e** exhibited the highest cytotoxicity toward representative cancer cell lines (nonadherent, human promyelocytic leukemia (HL-60), and adherent, human glioblastoma-astrocytoma (U373)). Interestingly, this prodrug was found to be not toxic toward nonmalignant cells (fibroblasts). We observed that with the exception of **1e** the cytotoxicity of the prodrugs correlates with their membrane permeability. Moreover, higher cytotoxicity is observed for the prodrugs releasing ferrocenium ions rather than iron ions. Both these trends provide us a rationale for future improvements of the properties of the aminoferrocene-based prodrugs.

EXPERIMENTAL SECTION

General Information. Commercially available chemicals of the best quality from Aldrich/Sigma/Fluka (Germany) were obtained and used without purification. NMR spectra were acquired on a Bruker Avance DRX 200, Bruker Avance II 400, or Bruker Avance III 600 spectrometer. ESI mass spectra were recorded on an ESI Q-tof Ultima API mass spectrometer (Waters), FAB mass spectra on a Jeol JMS-700 instrument using *p*-nitrobenzyl alcohol as a matrix, and EI mass spectra on a Finnigan MAT 8200 instrument. IR spectra were recorded on a Biorad Excalibur FTS 3000 instrument. The samples were prepared as KBr pellets. Cyclic voltamperometry was conducted on an EG&G 262A potentiostat/galvanometer. C, H, N analysis was performed in the microanalytical laboratory of the chemical institute of the University of Heidelberg. For analytical reversed-phase thin-layer chromatography, Polygram TLC plates (Macherey-Nagel) were used. UV/vis spectra were acquired on a Varian Cary 100 Bio UV/vis spectrophotometer by using 1 cm optical path black-wall absorption semimicrocuvettes (Hellma GmbH, Germany) with a sample volume of 0.7 mL. Fluorescence spectra were acquired on a Varian Cary Eclipse fluorescence spectrophotometer by using black-wall fluorescence semimicrocuvettes (Hellma GmbH) with a sample volume of 0.7 mL. The fluorescence of live HL-60 cells was quantified by using an Accuri C6 flow cytometer. The data were processed by using the CFlow Plus (Accuri) software package. The purity of the prodrugs used in the biological tests was determined by C, H, N analysis and thin-layer chromatography. According to these data, the prodrug samples were $\geq 95\%$ pure.

Synthesis. 4-(Hydroxymethyl)phenylboronic Acid Pinacol Ester. A suspension of 4-(hydroxymethyl)boronic acid (1.00 g, 6.6 mmol) and pinacol (0.79 g, 6.7 mmol) in THF (40 mL) was refluxed for 22 h. During this time the starting materials were completely dissolved. The solvent was removed in vacuum (10 mbar) and the residue redissolved in $\text{CH}_2\text{Cl}_2/\text{EtOAc}$ and purified by column chromatography on silica gel using a mixture of $\text{CH}_2\text{Cl}_2/\text{EtOAc}$ (9/1, v/v) as the eluent. Yield: 1.4 g (92%). $R_f = 0.3$ (silica, eluent $\text{CH}_2\text{Cl}_2/\text{EtOAc}$, 9/1, v/v). $^1\text{H NMR}$ (200 MHz, CDCl_3): δ (ppm)

1.35 (s, 12H), 4.71 (s, 2H), 7.37 (d, 2H, $^3J = 8.2$ Hz), 7.81 (d, 2H, $^3J = 8.2$ Hz).

4-[[[*N*-ferrocenylamino]carbonyl]oxy]methyl]phenylboronic Acid Pinacol Ester (prodrug **1a**). Aminoferrocene (1.20 g, 6.0 mmol) and triphosgene (1.80 g, 6.0 mmol) were added to dry toluene (110 mL) and purged with argon. The mixture was heated at 120 °C for 1 h. During this time all starting materials were dissolved. The solution obtained was cooled to 22 °C, and 4-(hydroxymethyl)phenylboronic acid pinacol ester (1.40 g, 6.0 mmol) dissolved in CH_2Cl_2 (150 mL) was added dropwise over 80 min. The solution was left stirring overnight at 22 °C. Then the solvent was removed in vacuum (10 mbar), and the product was purified by column chromatography on silica gel using CH_2Cl_2 as the eluent. Yield: 1.97 g (71%). $R_f = 0.3$ (silica, eluent CH_2Cl_2). $^1\text{H NMR}$ (400 MHz, include the list for acetone- d_6): δ (ppm) 1.33 (s, 12H), 3.95 (s, 2H), 4.12 (s, 5H), 4.59 (s, 2H), 5.17 (s, 2H), 7.42 (d, 2H), 7.76 (d, 2H). $^{13}\text{C NMR}$ (100.55 MHz, acetone- d_6): δ (ppm) 25.3, 61.1, 64.7, 66.5, 69.8, 84.6, 127.7, 127.8, 135.7, 141.4, 154.6. ESI TOF mass spectrometry (negative mode): m/z calcd for $[\text{M} - \text{pinacol} - \text{H}]^-$ ($\text{C}_{18}\text{H}_{17}\text{BFeNO}_4$) 378.07, found 378.04. Anal. Calcd for $\text{C}_{24}\text{H}_{28}\text{BFeNO}_4 \cdot 0.5\text{H}_2\text{O}$: C, 61.3; H, 6.2; N, 3.0. Found: C, 61.3; H, 5.9; N, 3.1.

4-(Hydroxymethyl)-2-fluorophenylboronic Acid. This compound was prepared according to the protocol described in ref 21 for analogous derivatives. Dimethylamine (1.9 mL of 2 M solution in THF, 3.7 mmol) was cooled to -78 °C. *n*-Butyllithium (1.7 mL of 1.6 M solution in hexane, 2.7 mmol) was added dropwise within 5 min. Next 4-bromo-3-fluorobenzyl alcohol (0.56 g, 2.7 mmol) dissolved in THF (1 mL) was slowly added while the temperature of the reaction mixture was kept at -78 °C. After the addition of the latter reagent and stirring for 5 min, the mixture was allowed to warm to room temperature (22 °C), and the solvent was removed in vacuum (10 mbar). The rest was redissolved in THF (10 mL) and cooled back to -78 °C. *n*-butyllithium (1.8 mL of 1.6 M solution, 2.8 mmol) was added within 5 min, and the mixture was allowed to react for 1 h while being stirred. Finally, triisopropyl borate (1.5 mL, 6.5 mmol) was added dropwise, and after 1 h the unreacted compounds were quenched with NaOH solution in water (5.1 mL, 1 M) and then with water (5.1 mL). After that, the mixture was warmed to 22 °C, all volatiles were removed in vacuum (10 mbar), and a mixture of water and diethyl ether was added. The aqueous phase was separated and acidified with concentrated HCl to pH 4. At these conditions the raw product was precipitated. It was purified by column chromatography on silica gel using $\text{CH}_2\text{Cl}_2/\text{EtOAc}$ (1/1, v/v) as the eluent. Yield: 0.90 g (99%). $R_f = 0.5$ (silica, eluent $\text{CH}_2\text{Cl}_2/\text{EtOAc}$, 1/1, v/v). $^1\text{H NMR}$ (200 MHz, D_2O): δ (ppm) 7.03 (m, 2H), 7.49 (m, 1H).

4-(Hydroxymethyl)-2-fluorophenylboronic Acid Pinacol Ester. 4-(Hydroxymethyl)-2-fluorophenylboronic acid (152 mg, 0.89 mmol) and pinacol (104 mg, 0.90 mmol) in tetrahydrofuran (17.2 mL) were refluxed for 3 h. The solvent was removed in vacuum (10 mbar), and the crude product obtained was purified by column chromatography on silica gel using $\text{CH}_2\text{Cl}_2/\text{EtOAc}$ (1/1, v/v) as the eluent. Yield: 115 mg (51%). $R_f = 0.7$ (silica, eluent $\text{CH}_2\text{Cl}_2/\text{EtOAc}$, 1/1, v/v). $^1\text{H NMR}$ (200 MHz, CDCl_3): δ (ppm) 1.36 (s, 12H), 4.71 (s, 2H), 7.08 (m, 2H), 7.71 (t, 1H, $^3J = 7.4$ Hz).

4-[[[*N*-ferrocenylamino]carbonyl]oxy]methyl]-2-fluorophenylboronic Acid Pinacol Ester (Prodrug **1b**). Aminoferrocene (82 mg, 0.4 mmol) and triphosgene (122 mg, 0.4 mmol) were added to dry toluene (7.5 mL) and purged with argon. The mixture was heated to 120 °C and kept at this temperature until all starting materials were dissolved. The solution obtained was cooled to 22 °C, and 4-(hydroxymethyl)-2-fluorophenylboronic acid pinacol ester (103 mg, 0.4 mmol) dissolved in CH_2Cl_2 (10 mL) was added dropwise. The solution was left stirring overnight at 22 °C. Then the solvent was removed in vacuum (10 mbar), and the product was purified by column chromatography on silica gel using hexane/EtOAc (8/2, v/v) as the eluent. Yield: 48 mg (24%). $R_f = 0.4$ (silica, eluent hexane/EtOAc, 8/2, v/v). $^1\text{H NMR}$ (200 MHz, acetone- d_6): δ (ppm) 1.34 (s, 12H), 3.94 (m, 2H), 4.11 (s, 5H), 4.56 (s, 2H), 5.19 (s, 2H), 7.13 (d, 1H), 7.23 (d, 1H), 7.71 (t, 1H). $^{13}\text{C NMR}$ (100.55 MHz, acetone- d_6): δ (ppm) 25.2, 61.1 (two overlapping signals), 64.7, 65.6, 69.8, 84.7,

114.9, 123.4, 137.9 (two overlapping signals), 166.9, 169.4. ^{19}F NMR (376.3 MHz, acetone- d_6): δ (ppm) -103.2 . FAB MS: m/z calcd for $\text{C}_{24}\text{H}_{27}\text{BFNO}_4\text{Fe}$ 479.1, found 479.1. Anal. Calcd for $\text{C}_{24}\text{H}_{27}\text{BFNO}_4\text{Fe}$ + acetone (one molecule of solvent): C, 60.8; H, 6.2; N, 2.6. Found: C, 60.4; H, 6.2; N, 2.6.

4-((Ferrocenylaminocarbonyl)oxymethyl)-2-methylphenylboronic acid pinacol ester (prodrug **1c**). Triphosgene (1.61 g, 5.44 mmol) and aminoferrocene (1.09 g, 5.44 mmol) were added to toluene (98 mL) and purged with argon. The mixture was heated up to 120 °C and kept at this temperature until all starting materials were dissolved (~30 min). The solution obtained was cooled down to 22 °C and 4-(hydroxymethyl)-2-methylphenylboronic acid pinacol ester (1.35 g, 5.44 mmol) dissolved in CH_2Cl_2 (132 mL) was added dropwise. The solution was left stirring at 22 °C for 44 h. Then, the solvent was removed in vacuum (10 mbar) and the product was purified by column chromatography on silica gel using hexane/EtOAc (10/2, v/v) as eluent. Yield: 0.83 g (32%). R_f = 0.33 (silica, eluent – $\text{CH}_2\text{Cl}_2/\text{EtOAc}$, 7/2, v/v). ^1H NMR (200 MHz, acetone- d_6): δ (ppm) 7.72 (d, 1H), 7.21 (m, 2H), 5.12 (s, 2H), 4.56 (s, 2H), 4.11 (s, 5H), 3.93 (s, 2H), 2.52 (t, 3H), 1.34 (s, 12H). ^{13}C NMR (100.55 MHz, acetone- d_6): δ (ppm) 145.8, 141.0, 137.0, 129.7, 124.7, 84.3, 69.8, 66.5, 64.7, 61.1, 25.3, 22.5. FAB MS: calculated for $\text{C}_{25}\text{H}_{30}\text{BFeNO}_4$ 475.2, found 475.2 m/z . C, H, N analysis: calculated for $\text{C}_{25}\text{H}_{30}\text{BFeNO}_4$ – C 63.2%; H 6.4%; N 3.0%; found – C 63.3%; H 6.6%; N 2.9%.

4-[[[(N-Ethyl-N-ferrocenylamino)carbonyl]oxymethyl]-2-phenylboronic Acid Pinacol Ester (Prodrug **1d**)]. Aminoferrocene (0.40 g, 1.98 mmol) and acetaldehyde (0.1 mL, 1.98 mmol) were dissolved in methanol (10 mL) and refluxed for 2 h. Then $\text{Na}[\text{B}(\text{CN})\text{H}_3]$ (0.12 g, 1.98 mmol) dissolved in MeOH (10 mL) was slowly added. The mixture obtained was acidified with HCl (2 mL, 1 M in water) and left stirring for 30 min. Afterward the solvent was removed in vacuum (0.01 mbar), and the rest was mixed with triphosgene (0.59 g, 1.98 mmol) in toluene (25 mL). The suspension obtained was refluxed for 1 h, cooled to 22 °C, and then mixed with a solution of 4-(hydroxymethyl)phenylboronic acid pinacol ester (0.46 g, 1.98 mmol) in toluene (10 mL). The resulting solution was heated to 120 °C and stirred at these conditions for 6 h. Then the solvent was removed in vacuum (0.01 mbar), and the crude product was purified by column chromatography on silica gel using hexane containing 5% acetone as the eluent. Yield: 0.20 g (20%). R_f = 0.5 (silica, eluent hexane/acetone, 5/1, v/v). ^1H NMR (400 MHz, acetone- d_6): δ (ppm) 1.27 (t, 3H), 1.33 (s, 12H), 3.77 (q, 2H), 4.00 (s, 2H), 4.13 (s, 5H), 4.53 (m, 2H), 5.22 (s, 2H), 7.46 (d, 1H), 7.77 (d, 2H). ^{13}C NMR (100.55 MHz, acetone- d_6): δ (ppm) 14.4, 25.3, 45.8, 62.8, 65.1, 66.9, 67.5, 69.8, 84.6, 127.8, 128.1, 135.7 (two overlapping peaks), 139.1, 141.2. EI MS: m/z calcd for $\text{C}_{26}\text{H}_{32}\text{BNO}_4\text{Fe}$ 489.2, found 489.2. IR spectra (in KBr): wavenumber (cm^{-1}) 3101, 2973, 1696, 1623. Anal. Calcd for $\text{C}_{26}\text{H}_{32}\text{BNO}_4\text{Fe}$: C, 63.8; H, 6.6; N, 2.9%. Found: C, 63.8; H, 6.8; N, 2.9.

4-[[[(N-Benzyl-N-ferrocenylamino)carbonyl]oxy]methyl]-2-phenylboronic Acid Pinacol Ester (Prodrug **1e**). Compound **1e** was obtained analogously to **1d** except that benzaldehyde (0.2 mL, 1.98 mmol) was used in place of acetaldehyde. Yield: 60 mg (5%). R_f = 0.4 (silica, eluent hexane/acetone, 5/1, v/v). ^1H NMR (400 MHz, acetone- d_6): δ (ppm) 1.33 (s, 12H), 3.97 (s, 2H), 4.11 (s, 5H), 4.45 (s, 2H), 5.02 (s, 2H), 5.52 (s, 2H), 7.34 (m, 7H), 7.72 (m, 2H). ^{13}C NMR (100.55 MHz, acetone- d_6): δ (ppm) 25.3, 53.9, 63.4, 65.1, 67.6, 67.9, 69.8, 84.6, 127.3 (two overlapping peaks), 127.8, 127.9, 129.4, 135.7, 140.0, 141.0, 142.5. EI MS: m/z calcd for $\text{C}_{31}\text{H}_{34}\text{BNO}_4\text{Fe}$ 551.2, found 551.2. IR spectra (in KBr): wavenumber (cm^{-1}) 3070, 2973, 1700, 1623. Anal. Calcd for $\text{C}_{31}\text{H}_{34}\text{BNO}_4\text{Fe}$: C, 67.5; H, 6.2; N, 2.5. Found: C, 67.4; H, 6.5; N, 2.5.

In Vitro Assays. *Monitoring Release of Iron Ions from the Prodrugs and Control Compounds in the Presence of Hydrogen Peroxide.* A solution of a ferrocene complex (10 μL , 10 mM in DMF containing 2% water and 1% sodium ascorbate) was diluted with MOPS buffer (990 μL , 100 mM, pH 7.5). Such probes were incubated with H_2O_2 (stock solutions of different concentrations (1 μL) were added) at 22 °C for selected time periods. Then the reaction was quenched by adding sodium dithionite (20 μL , 1 M in water), which

converts Fe^{3+} into Fe^{2+} . Finally, 2,2'-bipyridine solution (3 μL , 100 mM in DMF) was added to form a dark red $[\text{Fe}(\text{2,2}'\text{-bipyridine})_3]^{2+}$ complex ($\lambda_{\text{max}} = 519 \text{ nm}$). FeSO_4 sulfate (100 μM) was used as a positive control to determine the absorbance intensity when the ferrocene complexes were completely converted by H_2O_2 to free Fe^{2+} . The efficacy of iron release from a prodrug in the presence of H_2O_2 (the data are provided in Table 2) was determined by using the following formula: iron release efficacy = $(A_{519 \text{ nm}}(\text{prodrug}) - A_{519 \text{ nm}}(\text{buffer})) / (A_{519 \text{ nm}}(\text{FeSO}_4) - A_{519 \text{ nm}}(\text{buffer}))$, where $A_{519 \text{ nm}}(\text{prodrug})$ is the absorbance at 519 nm of a prodrug treated with H_2O_2 (1 mM) for 100 min and then with 2,2'-bipyridine as described above, $A_{519 \text{ nm}}(\text{FeSO}_4)$ is the absorbance at 519 nm of FeSO_4 solution treated in a similar way, and $A_{519 \text{ nm}}(\text{buffer})$ is the absorbance at 519 nm of the buffer treated analogously.

Reversed-Phase Thin-Layer Chromatography for Monitoring Decomposition of 1a. Three probes were analyzed by reversed-phase TLC using plates covered with C18-modified silica (ALUGRAM RP-18W, Macherey-Nagel) and 1/1 (v/v) DMF/MOPS buffer (100 mM, pH 7.5) as the eluent. The first probe was prodrug **1a** (10 mM) dissolved in DMF containing 2% water. The second one was prodrug **1a** (10 mM) dissolved in the same solvent treated with excess H_2O_2 (100 mM) for 24 h. The third probe was 4-(hydroxymethyl)phenol (**8a**; 10 mM) also dissolved in DMF containing 2% water. At these conditions R_f of phenol **8a** was found to be 0.80, whereas that of prodrug **1a** was found to be 0.08. In the TLC of **1a** treated with H_2O_2 , the spot corresponding to the intact prodrug was not observed whereas the intense spot at $R_f = 0.80$ corresponding to phenol **8a** was detected (Figure S13, Supporting Information). In the TLC of **1a** treated with H_2O_2 for 30 min, another spot at $R_f = 0.4$ was also observed (data not shown). According to ESI MS analysis, this product could be identified as compound **2a**, which is formed as a result of cleavage of the B–C bond in **1a** (Scheme 2).

Monitoring Generation of ROS by Using Fluorescence Spectroscopy. 2',7'-Dichlorofluorescein diacetate (DCFH-DA; 4.9 mg) was dissolved in DMF (100 μL) and mixed with aqueous NaOH (0.1 M, 900 μL). The resulting mixture was incubated for 30 min at 22 °C in the dark to obtain a stock solution of 2',7'-dichlorofluorescein (DCFH; 10 mM). Next a solution (1 mL) containing DCFH (10 μM), MOPS buffer (100 mM, pH 7.5), EDTA (10 mM), glutathione (5 mM), and H_2O_2 (10 mM) was prepared. Monitoring of the fluorescence ($\lambda_{\text{ex}} = 501 \text{ nm}$, $\lambda_{\text{em}} = 531 \text{ nm}$) of this solution was started. After 5 min, an iron complex (100 μM , ferrocene prodrugs **1a–e**, positive or negative controls) was added, and the fluorescence monitoring was continued until the fluorescence signal growth was stalled. The efficacy of ROS generation (the data are provided in Table 2) was determined using the following formula: efficacy = $(F(\text{prodrug}) - F_0) / (F(\text{FeSO}_4) - F_0)$, where $F(\text{prodrug})$ is the fluorescence of the DCFH mixture treated with a prodrug for 17 min, $F(\text{FeSO}_4)$ is the fluorescence of the same mixture treated with FeSO_4 for 17 min, and F_0 is the fluorescence of a mixture containing no iron complex.

CV Measurements. The concentration of iron complexes tested was 1 mM. Measurements were conducted at 22 °C. Ag/AgCl was used as a reference electrode. The supporting electrolyte in experiments conducted in pure DMF was tetramethylammonium hexafluorophosphate (160 mM). The aqueous buffer was phosphate-buffered saline (PBS) buffer (phosphate, 9.5 mM; NaCl, 137.9 mM; KCl, 2.7 mM) containing 50% DMF (v/v).

Cellular Assays. *Cells and Cell Culture.* The human glioblastoma-astrocytoma cell line (U373) was cultured in Eagle's minimum essential medium (EMEM) supplemented with 10% fetal calf serum (FCS), 1% L-glutamine, and 1% penicillin/streptomycin. The human promyelocytic leukemia cell line (HL60) was cultured in Roswell Park Memorial Institute (RPMI) 1640 medium supplemented with 10% FCS and 5 $\mu\text{g}/\text{mL}$ penicillin/streptomycin (all media and supplements from Gibco Invitrogen Corp., Karlsruhe, Germany). Fibroblasts were grown in DMEM (Dulbecco's modified Eagle's medium) supplemented with 10% FCS, 1% L-glutamine, and 1% penicillin/streptomycin.

Assay for Determination of Cell Permeability of the Prodrugs (Table 2) (According to the Protocol Described in Ref 28). HL60-

cells grown in RPMI 1640 medium supplemented with 10% FCS, 1% glutamine, and 1% penicillin/streptomycin were centrifuged, and the medium was replaced with RPMI 1640 medium (5% FCS, 1% L-glutamine, 1% penicillin/streptomycin) to obtain suspensions containing 10^6 cells/mL. Solutions of prodrugs (5 μ L, solvent DMF containing 2% water and 1% sodium ascorbate) were added to the suspensions (500 μ L) and incubated for 1 h. The final concentration of the prodrugs in the suspensions was 100 μ M. Then the cells were washed three times with PBS buffer (3 \times 500 μ L) and treated with concentrated H₂O₂ solution (200 μ L, 1 M) for 30 min, and all volatiles were removed by lyophilization. Dry, lysed cells were washed with water (200 μ L), and aqueous solution obtained was acidified with HCl (400 μ L, 0.1 M). Then this solution was extracted with 2-ethyl-1,3-hexanediol (100 μ L, 10% in CHCl₃, v/v), and a portion of the organic phase obtained (40 μ L) was mixed with H₂SO₄/CH₃CO₂H (400 μ L, 1/1, v/v). Curcumin solution in methyl isobutyl ketone (500 μ L, 2 mg in 1 mL of the solvent) was added and allowed to react for 24 h. The reaction was quenched by addition of water (1 mL). Light absorbances at 550 and 780 nm of the organic phase were measured. The value $A(550 \text{ nm}) - A(780 \text{ nm})$ was proportional to the concentration of boron in the mixture. The amount of boron released from prodrug **1a** was taken as a reference. All other values were determined relative to this reference.

Estimation of Oxidative Stress in Live HL-60 Cells. An aliquot of the HL-60 cells was taken from the cultivation medium (RPMI 1640 supplemented with 10% FCS, 1% L-glutamine, and 1% penicillin/streptomycin). The medium was replaced with PBS buffer to obtain a cell suspension with 10^6 cells/mL. DCFH-DA solution (1 μ L, 10 mM in DMSO) was added to the suspension (1 mL) and incubated in the dark chamber filled with CO₂ (5%) at 37 °C for 5 min. Then the cells were washed with PBS, and iron complexes (10 μ L of stock solutions, solvent DMF containing 2% water and 1% sodium ascorbate, final concentration of the complex 100 μ M) in Opti-MEM medium were added. After 30 min of incubation in the dark chamber filled with CO₂ (5%) at 37 °C, the cells were washed with Opti-MEM medium and left standing at 20 °C for 4.5 h. After that the fluorescence of live cells ($\lambda_{\text{ex}} = 488 \text{ nm}$, $\lambda_{\text{em}} = 530 \text{ nm}$) in the suspensions was determined by using the flow cytometer. The relative efficacy of ROS generation of the prodrugs (**1a–e**) as well as of negative control **10** was calculated using the formula efficacy = $F(\text{prodrug})/F_0$, where $F(\text{prodrug})$ is the mean fluorescence intensity of cells incubated with a prodrug and treated as described above and F_0 is the mean fluorescence intensity of cells which were not treated with any iron complex.

Assay for Determination of the Viability of Adherent Cells (MTT Assay). Adherent U373 cells were grown in EMEM supplemented with 10% FCS, 1% L-glutamine, and 1% penicillin/streptomycin to 80–90% confluence. Then the medium was removed, and the cells were washed two times with PBS buffer, trypsinated, and resuspended in the RPMI 1640 medium containing 1% FCS, 1% L-glutamine, and 1% penicillin/streptomycin. This suspension was spread in the wells of a 96-well microtiter plate (~25 000 cells per well per 100 μ L) and left standing at 37 °C in the chamber filled with CO₂ (5%) for 5 h. Stock solutions of prodrugs of different concentrations (1 μ L, solvent DMF containing 2% water and 1% sodium ascorbate) were added to the wells and incubated for specific periods of time. Four experiments were conducted for each concentration of the prodrug. Finally, 3-(4,5-dimethylthiazol-2-yl)-2,5-diphenyltetrazolium bromide (MTT; 20 μ L of the solution prepared by dissolving MTT (5 mg) in PBS buffer (1 mL) was added to each well, incubated for 3 h, treated with sodium dodecyl sulfate (SDS) solution (90 μ L, 10% solution in 0.01 M aqueous HCl), and incubated overnight. Then the intensity of absorbance at 590 nm was measured (MTT is converted to blue dye ($\lambda_{\text{max}} = 590 \text{ nm}$) in live cells). The absorbance at 690 nm was taken as a baseline value. These data were applied to calculate the relative number of viable cells.

Assay for Determination of the Viability of Nonadherent Cell Lines (PI Assay). HL-60 cells grown in RPMI 1640 medium supplemented with 10% FCS, 1% L-glutamine, and 1% penicillin/streptomycin were centrifuged, and the medium was replaced with RPMI 1640 medium (5% FCS, 1% L-glutamine, 1% penicillin/

streptomycin) to obtain suspensions containing 10^6 cells/mL. Stock solutions of prodrugs of different concentrations (5 μ L, solvent DMF containing 2% water and 1% sodium ascorbate) were added to the cellular suspensions (500 μ L) and incubated for specific periods of time. Four experiments were conducted for each concentration of the prodrug. At the end of the incubation period, propidium iodide (PI; 1 μ L, 1.5 mM in water) was added to label leaky cells, and in 5 min the suspension of the cells was analyzed by using flow cytometry.

■ ASSOCIATED CONTENT

📄 Supporting Information

¹H and ¹³C NMR spectra of new prodrugs, monitoring reaction of prodrug **1a** with H₂O₂ by using reversed-phase TLC, release of iron ions from prodrug **1a** in the presence of different reactive oxygen species, evaluation of oxidative stress in HL-60 cells and fibroblasts in the absence and presence of prodrug **1e**, and description of cellular assays. This material is available free of charge via the Internet at <http://pubs.acs.org>.

■ AUTHOR INFORMATION

Corresponding Author

*E-mail: Andriy.Mokhir@urz.uni-heidelberg.de. Phone: +49-6221-548441. Fax: 49-06221-548439.

Author Contributions

[§]These authors contributed equally to this work.

■ ACKNOWLEDGMENTS

We thank Prof. Dr. Peter Comba and Dr. Bodo Martin (Ruprecht-Karls-University of Heidelberg) for discussions of the mechanism of oxidative decomposition of aminoferrocenes. The funding for this project was provided by Ruprecht-Karls-University Heidelberg and Bernthsen-Stiftung.

■ ABBREVIATIONS USED

azpy, 2-(phenylazo)pyridine; Bipy, 2,2'-bipyridine; Cp, cyclopentadienyl; EDTA, N,N,N',N'-ethylenediaminetetraacetic acid; Fc, ferrocene; Fc⁺, ferrocenium; GSH, reduced glutathione; GSSG, oxidized glutathione; HL-60, human promyelocytic leukemia cells; HL-60cat, human promyelocytic leukemia cells overexpressing catalase; 8-HQ, 8-hydroxyquinoline; HT29, human colon adenocarcinoma cells; MDA-MB-231, human breast adenocarcinoma cells; MMP, matrix metalloprotease; MOPS, 3-(N-morpholino)propanesulfonic acid; MTT, 3-(4,5-dimethylthiazol-2-yl)-2,5-diphenyltetrazolium bromide; NO-ASA, nitric oxide-donating aspirin; QM, quinone methide; ROS, reactive oxygen species; SW480, human colon adenocarcinoma cells; U373, human glioblastoma-astrocytoma cells

■ REFERENCES

- (1) Jung, Y.; Lippard, S. J. Direct cellular responses to platinum-induced DNA damage. *Chem. Rev.* **2007**, *107*, 1387–1407.
- (2) Galmarini, C. M.; Mackey, J. R.; Dumontet, G. Nucleoside analogues and nucleobases in cancer treatment. *Lancet Oncol.* **2002**, *3*, 415–424.
- (3) (a) Halliwell, B. Oxidative stress and cancer: have we moved forward? *Biochem. J.* **2007**, *401*, 1–11. (b) Engel, R. H.; Evens, A. M. Oxidative stress and apoptosis: a new treatment paradigm in cancer. *Front. Biosci.* **2006**, *11*, 300–312. (c) Finkel, T. Oxidant signals and oxidative stress. *Curr. Opin. Cell Biol.* **2003**, *15*, 247–254. (d) Schumacker, P. T. Reactive oxygen species in cancer cells: live by the sword, die by the sword. *Cancer Cell* **2006**, *10*, 175–176. (d) Antunes, F.; Cadenas, R. Estimation of H₂O₂ gradients across biomembranes. *FEBS Lett.* **2000**, *475*, 121–126. (e) Szatrowski, T. P.;

Nathan, C. F. Production of large amounts of hydrogen peroxide by human tumor cells. *Cancer Res.* **1991**, *51*, 794–798. (f) O'Donnell-Tormey, J.; DeBoer, C. J.; Nathan, C. F. Resistance of human tumor cells in vitro to oxidative cytolysis. *J. Clin. Invest.* **1985**, *76*, 80–86. (g) Stone, J. R. An assessment of proposed mechanisms for sensing hydrogen peroxide in mammalian systems. *Arch. Biochem. Biophys.* **2004**, *422*, 119–124.

(4) Davison, K.; Mann, K. K.; Miller, W. H. Arsenic trioxide: mechanisms of action. *Semin. Hematol.* **2002**, *39* (Suppl. 1), 3–7.

(5) (a) Dorr, R. T.; Liddell, J. D.; Soble, M. J. Cytotoxic effects of glutathione-synthesis inhibition by L-buthionine-(S,R)-sulfoximine on human and murine tumor cells. *Invest. New Drugs* **1986**, *4*, 305–313. (b) Renschler, M. F. The emerging role of reactive oxygen species in cancer therapy. *Eur. J. Cancer* **2004**, *40*, 1934–1940.

(6) Trachootham, D.; Zhou, Y.; Zhang, H.; Demizu, Y.; Chen, Z.; Pelicano, H.; Chiao, P. J.; Achanta, G.; Arlinghaus, R. B.; Liu, J.; Huang, P. Selective killing of oncogenically transformed cells through a ROS-mediated mechanism by β -phenylethyl isothiocyanate. *Cancer Cell* **2006**, *10*, 241–252.

(7) Hulsman, N.; Medema, J. P.; Bos, C.; Jongejan, A.; Leurs, R.; Smit, M. J.; de Esch, I. J. P.; Richel, D.; Wijtman, M. Chemical insights in the concept of hybrid drugs: the antitumor effect of nitric oxide-donating aspirin involves a quinone methide but not nitric oxide nor aspirin. *J. Med. Chem.* **2007**, *50*, 2424–2431.

(8) Magda, D.; Lepp, C.; Gerasimchuk, N. N.; Lee, I.; Sessler, J. L.; Lin, A.; Bioglow, J. E.; Miller, R. A. Redox cycling by motexafin gadolinium enhances cellular response to ionizing radiation by forming reactive oxygen species. *Int. J. Radiat. Oncol., Biol., Phys.* **2001**, *51*, 1025–1036.

(9) (a) Köpf-Maier, P.; Köpf, H.; Neuse, E. W. J. Ferricenium complexes: a new type of water-soluble antitumor agent. *Cancer Res. Clin. Oncol.* **1984**, *108*, 336–340. (b) Köpf-Maier, P.; Köpf, H. Non-platinum group metal antitumor agents. History, current status, and perspectives. *Chem. Rev.* **1987**, *1137*–1152. (c) van Staveren, D. R.; Metzler-Nolte, N. Bioorganometallic chemistry of ferrocene. *Chem. Rev.* **2004**, *104*, 5931–5985.

(10) Dougan, S. J.; Habtemariam, A.; McHale, S. E.; Parsons, S.; Sadler, P. J. Catalytic organometallic anticancer complexes. *Proc. Natl. Acad. Sci. U.S.A.* **2008**, *105*, 11628–11633.

(11) (a) Totter, J. R. Spontaneous cancer and its possible relationship to oxygen metabolism. *Proc. Natl. Acad. Sci. U.S.A.* **1980**, *77*, 1763–1767. (b) Beckman, K. B.; Ames, B. N. Oxidative decay of DNA. *J. Biol. Chem.* **1997**, *272*, 19633–19636.

(12) (a) Hamels, D.; Dansette, P. M.; Hillard, E. A.; Top, S.; Vessieres, A.; Herson, P.; Jaouen, G.; Mansuy, D. Ferrocenyl quinone methides as strong antiproliferative agents: formation by metabolic and chemical oxidation of ferrocenyl phenols. *Angew. Chem., Int. Ed.* **2009**, *48*, 9124–9126. (b) Jaouen, G.; Top, S.; Vessieres, A. Organometallics targeted to specific biological sites: the development of new therapies. In *Bioorganometallics*; Jaouen, G., Ed.; Wiley-VCH: Weinheim, Germany, 2006; p 65. (c) Hillard, E. A.; Vessieres, A.; Thouin, L.; Jaouen, G.; Amatore, C. Ferrocene-mediated proton-coupled electron transfer in a series of ferrocifen-type breast-cancer drug candidates. *Angew. Chem., Int. Ed.* **2006**, *45*, 285–290.

(13) (a) Khosrow, K.; Rigas, B. The mechanism of action of nitric oxide-donating aspirin. *Biochem. Biophys. Res. Commun.* **2007**, *358*, 1096–1101.

(14) Wlassoff, W. A.; Albright, C. D.; Sivashinski, M. S.; Ivanova, A.; Appelbaum, J. G.; Salganik, R. I. Hydrogen peroxide overproduced in breast cancer cells can serve as an anticancer prodrug generating apoptosis-stimulating hydroxyl radicals under the effect of tamoxifen-ferrocene conjugate. *J. Pharm. Pharmacol.* **2007**, *59*, 1549–1553.

(15) Pigeon, P.; Top, S.; Vessières, A.; Huchè, M.; Görmen, M.; El Arbi, M.; Plamont, M.-A.; McGlinchey, M. J.; Jaouen, G. A new series of ferrocifen derivatives, bearing two aminoalkyl chains, with strong antiproliferative effects on breast cancer cells. *New J. Chem.* **2011**, *35*, 2212–2218.

(16) (a) Charkoudian, L. K.; Pham, D. M.; Franz, K. J. A pro-chelator triggered by hydrogen peroxide inhibits iron-promoted hydroxyl

radical formation. *J. Am. Chem. Soc.* **2006**, *128*, 12424–12425. (b) Wei, Y.; Guo, M. Hydrogen peroxide triggered pro-chelator activation, subsequent metal chelation, and attenuation of the Fenton reaction. *Angew. Chem., Int. Ed.* **2007**, *46*, 4722–4725. (c) Major Jourden, J. L.; Cohen, S. M. Hydrogen peroxide activated matrix metalloproteinase inhibitors: a prodrug approach. *Angew. Chem., Int. Ed.* **2010**, *49*, 6795–6797.

(17) (a) Folk, D. S.; Franz, K. J. A pro-chelator activated by β -secretase inhibits A β aggregation and suppresses copper-induced reactive oxygen species formation. *J. Am. Chem. Soc.* **2010**, *132*, 4994–4995. (b) Schugar, H.; Green, D. E.; Bowen, M. L.; Scott, L. E.; Storr, T.; Bohmerle, K.; Thomas, F.; Allen, D. D.; Lockman, P. R.; Merkel, M.; Thompson, K. H.; Orvig, C. Combating Alzheimer's disease with multifunctional molecules designed for metal passivation. *Angew. Chem., Int. Ed.* **2007**, *46*, 1716–1718.

(18) McDonnell, S. O.; Hall, M. J.; Allen, L. T.; Byrne, A.; Gallagher, W. M.; O'Shea, D. F. Supramolecular photonic therapeutic agents. *J. Am. Chem. Soc.* **2005**, *127*, 16360–16361.

(19) Goldstein, S.; Meyerstein, D.; Czapski, G. The Fenton reagents. *Free Radical Biol. Med.* **1993**, *15*, 435–445.

(20) Trachootham, D.; Alexandre, J.; Huang, P. Targeting cancer cells by ROS-mediated mechanisms: a radical therapeutic approach? *Nat. Rev. Drug Discovery* **2009**, *8*, 579–591.

(21) Zheng, N.; Armstrong, J. D.; Eng, K. K.; Keller, J.; Liu, T.; Purick, R.; Lynch, J.; Hartner, F. W.; Volante, R. P. A convergent asymmetric synthesis of a growth hormone secretagogue. *Tetrahedron: Asymmetry* **2003**, *14*, 3435–3446.

(22) Heinze, K.; Schlenker, M. Main chain ferrocenyl amides from 1-amino-1'-carboxyferrocene. *Eur. J. Inorg. Chem.* **2004**, 2974–2988.

(23) Knox, G. R.; Pauson, P. L. 903. Ferrocene derivatives. Part XI. Azoferrocenes. *J. Chem. Soc.* **1961**, 4615–4618.

(24) *The IUPAC Stability Constants Database*; SCQuery Vn 4.06/4.045, Academic Software: Sourby Old Farm, Timble, Otley, Yorks, LS21 2PW, UK.

(25) Britton, W. E.; Kashyap, R.; El-Hashash, M.; El-Kady, M. The anomalous electrochemistry of the ferrocenylamines. *Organometallics* **1986**, *5*, 1029–1031.

(26) Sohn, Y. S.; Hendrickson, D. N.; Grey, H. B. Electronic structure of metallocenes. *J. Am. Chem. Soc.* **1971**, *93*, 3603–3612.

(27) Dutta, S.; Mokhir, A. An autocatalytic, chromogenic and fluorogenic photochemical reaction controlled by nucleic acids. *Chem. Commun.* **2011**, *47* (4), 1243–1245.

(28) Wimmer, M. A.; Goldbach, H. E. A miniaturized curcumin method for the determination of boron in solutions and biological samples. *J. Plant Nutr. Soil Sci.* **1999**, *162*, 15–18.

(29) Ma, Y.; Liu, Z.; Hider, R. C.; Petrat, F. Determination of the labile iron pool of human lymphocytes using the fluorescent probe, CP655. *Anal. Chem. Insights* **2007**, *2*, 61–67.